

Published in final edited form as:

J Mol Biol. 2009 November 27; 394(2): 297–305. doi:10.1016/j.jmb.2009.09.023.

Reconstitution and Engineering of Apoptotic Protein Interactions on the Bacterial Cell Surface

Jingjing Sun¹, Diya M. Abdeljabbar¹, Nicole Clarke¹, Meghan L. Bellows¹, Christodoulos A. Floudas¹, and A. James Link^{1,2,*}

¹ Department of Chemical Engineering, Princeton University, Princeton, NJ 08544, USA

² Department of Molecular Biology, Princeton University, Princeton, NJ 08544, USA

Abstract

The interactions between pro- and anti-apoptotic members of the Bcl-2 class of proteins control whether a cell lives or dies, and the study of these protein–protein interactions has been an area of intense research. In this report, we describe a new tool for the study and engineering of apoptotic protein interactions that is based on the flow cytometric detection of these interactions on the surface of *Escherichia coli*. After validation of the assay with the well-studied interaction between the Bak(72–87) peptide and the anti-apoptotic protein Bcl-x_L, the effect of both increasing and decreasing Bak peptide length on Bcl-x_L binding was investigated. Previous work demonstrated that the Bak(72–87) peptide also binds to the anti-apoptotic protein Bcl-2, albeit with lower binding affinity compared to Bcl-x_L. Here, we demonstrate that a slightly longer Bak peptide corresponding to amino acids 72–89 of Bak binds Bcl-x_L and Bcl-2 equally well. Approximate binding affinity calculations on these peptide–protein complexes confirm the experimental observations. The flow cytometric assay was also used to screen a saturation mutagenesis library of Bak(72–87) variants for improved affinity to Bcl-x_L. The best variants obtained from this library exhibit an apparent K_d to Bcl-x_L 4-fold lower than that of wild-type Bak(72–87).

Keywords

apoptosis; protein–protein interactions; cell surface display; Bcl-2 proteins

Introduction

The Bcl-2 class of proteins is critical to the regulation of apoptosis.^{1–3} Though all members of the class exhibit similar α -helical tertiary structures, the class can be further divided, on the basis of function, into pro-apoptotic and anti-apoptotic subclasses.⁴ Pro-apoptotic Bcl-2 proteins, such as Bak and Bax,^{5,6} initiate cell death while anti-apoptotic proteins, including Bcl-2 and Bcl-x_L, prevent cell death.^{7,8} Bak and Bax promote cell death by permeabilizing the mitochondrial membrane, leading to the release of cytochrome *c* into the cytoplasm^{9,10} and ultimately activation of caspases.¹¹ One mechanism by which anti-apoptotic subclass members prevent apoptosis is the formation of heterodimers of anti-apoptotic proteins with Bak or Bax, thus sequestering these pro-apoptotic proteins.¹² Since elevated levels of Bcl-2 and Bcl-x_L are found in several cancers,^{7,13–18} much effort has been put into understanding

*Corresponding author. Department of Chemical Engineering, A207 Engineering Quadrangle, Princeton University, Princeton, NJ 08544, USA. ajlink@princeton.edu.

Supplementary Data

Supplementary data associated with this article can be found, in the online version, at doi:10.1016/j.jmb.2009.09.023.

the heterodimeric interactions between pro- and anti-apoptotic Bcl-2 class members. These protein–protein interactions have been extensively studied through structural biology efforts,^{19–22} *in vitro* binding assays,^{19,23–25} and *in vivo* techniques such as co-immunoprecipitation.^{5,26} It has been established that binding between Bak and Bcl-x_L is mediated by the amphipathic α -helix corresponding to the BH3 homology region of Bak, which, when complexed, resides in a hydrophobic cleft of Bcl-x_L.¹⁹ A 16-amino-acid peptide corresponding to the BH3 region (residues 72–87) of Bak is sufficient for binding to Bcl-x_L.¹⁹ This same peptide binds to Bcl-2 but with a lower affinity,²³ leading to the conclusion that Bak has some specificity toward Bcl-x_L relative to Bcl-2.²⁷

In this work, we sought to develop a recombinant system for examining Bak peptide–Bcl-x_L interactions rapidly and quantitatively to investigate the role of Bak peptide length on its binding to Bcl-x_L and Bcl-2. To this end, we have recapitulated the interaction between the Bak BH3 peptide and Bcl-x_L on the cell surface of *Escherichia coli* (Fig. 1). Bacterial cell surface display has been successfully employed previously for the study and engineering of biomolecular interactions,²⁸ including the selection of peptides with binding capability from large random libraries²⁹ and antibody affinity maturation.^{30,31} In our binding platform, the Bak peptide is fused to the N-terminus of the enhanced circularly permuted OmpX (eCPX) display protein,^{32,33} thus decorating the cell surface with many copies of the Bak peptide. Subsequent binding steps with biotinylated Bcl-x_L and fluorescent streptavidin render cells with productive binding fluorescent, allowing quantitative detection of the binding event by flow cytometry. Combining this platform with cell sorting allows the screening of combinatorial libraries of Bak variants for improved affinity to Bcl-x_L. Herein, we validate our binding platform with a previously studied Bak peptide, Bak(72–87), and systematically evaluate the effects of changing the length of the Bak peptide on its binding to Bcl-x_L and the related protein Bcl-2. In addition, we identify and characterize variants of the Bak(72–87) peptide with improved apparent affinity to Bcl-x_L by screening a saturation mutagenesis library of Bak variants.

Results and Discussion

Recapitulation of Bak(72–87)–Bcl-x_L binding on the *E. coli* cell surface

As an initial qualitative validation of the surface-displayed Bak binding platform (Fig. 1), the peptide corresponding to amino acids 72–87 of Bak was fused to the N-terminus of the eCPX display vehicle. To ensure saturation binding, we treated cells displaying the Bak(72–87)–eCPX fusion with 1.66 μ M Bcl-x_L, a concentration several-fold higher than the K_d previously determined for the Bak(72–87)–Bcl-x_L interaction (340 nM).¹⁹ Following staining with streptavidin–phycoerythrin (SAPE), cells displaying the peptide exhibit a median fluorescence about 15-fold higher than that of cells displaying an eCPX protein with no peptide fused to its N-terminus (Fig. 2). A critical leucine in position 78 of the Bak peptide was changed to alanine (L78A) to ensure that the increase in fluorescence observed was due to binding of the Bak peptide and Bcl-x_L. It has been previously demonstrated that this amino acid change leads to a nearly 1000-fold decrease in the binding affinity of Bak(72–87) for Bcl-x_L.^{19,25} We observe that cells displaying this mutant peptide have only background fluorescence following treatment with Bcl-x_L and SAPE (Fig. 2). Collectively, these results illustrate that our binding platform can qualitatively capture Bak(72–87)–Bcl-x_L binding behavior.

As a more stringent validation of the platform, we generated a binding isotherm for the Bak(72–87)–Bcl-x_L interaction by incubating cells displaying Bak (72–87) with concentrations of Bcl-x_L ranging from 1.6 nM to 8 μ M and measuring the median fluorescence intensity of the resulting cell populations using flow cytometry (Fig. 3a). The data were fit to a single-site saturation model that takes into account binding site depletion

(see Supplementary Materials and Methods for model details). The data fit a simple single-site saturation model equally well (Fig. S1) and permit an estimation of the value of K_d . The value of K_d we measured, 204 nM, is in reasonable agreement with the K_d of 340 nM previously measured with purified components by a fluorescence assay.¹⁹ A K_d value of 480 nM for the Bak(72–87)–Bcl-x_L interaction was determined using fluorescence polarization assays.²³

In addition to determining the equilibrium dissociation constant, K_d , the individual rate constants for association and dissociation (k_{on} and k_{off} , respectively) were estimated using a competition assay. Following equilibrium binding of cells displaying Bak(72–87) with Bcl-x_L and SAPE staining, a large excess (41.5 μM) of non-biotinylated Bcl-x_L was added to the cells, and the median fluorescence of the cell population was monitored as a function of time. Fitting of these data to a first-order exponential decay model led to an estimate of $k_{off} = 1.42 \times 10^{-3} \text{ s}^{-1}$ and $k_{on} = 6.97 \times 10^3 \text{ M}^{-1} \text{ s}^{-1}$ (Fig. 3b), where k_{on} is calculated using the value of K_d we measured, 204 nM. To our knowledge, these rate constants have not been reported [for instance, by surface plasmon resonance (SPR) measurements] for this particular peptide–protein pair, though SPR has been employed to determine these kinetic parameters for the related Bim peptide–Bcl-2 interaction.²⁴ The values we estimate for k_{on} and k_{off} are similar in magnitude to those measured by SPR for the Bim–Bcl-2 interaction. SPR measurements have also been carried out to determine the equilibrium dissociation constant of the interaction between Bcl-x_L and a longer Bak peptide, Bak(67–92), but the individual k_{on} and k_{off} parameters were not reported.²⁵

Effect of Bak peptide length on Bcl-x_L binding

After determining that the surface display system could effectively capture the binding between the Bak(72–89) peptide and Bcl-x_L, we next turned our attention to the effect of increasing the length of the Bak peptide. Several eCPX–Bak fusions were constructed based upon secondary-structure elements of the full Bak protein (Fig. 4).³⁴ The BH3 region of Bak is contained within a longer, kinked helix, α_3 , composed of residues 70–98. Equilibrium binding of Bcl-x_L to a peptide composed of residues 70–93 of Bak resulted in fluorescence slightly lower than that observed for the Bak(72–87) peptide (Table 1). However, fusion proteins comprising helices α_1 , α_2 , and α_3 [Bak(24–89)] or helices α_3 and α_4 [Bak(72–117)] exhibited fluorescence only slightly above background levels in equilibrium binding experiments. A construct containing amino acids 24–117 of Bak (comprising helices α_1 to α_4) also exhibited essentially no binding to Bcl-x_L as judged by our assay. Western blotting experiments on outer-membrane protein preparations (OMPs) confirm that all of the constructs except Bak(24–117) are expressed and targeted efficiently to the outer membrane (Fig. S2). Given that the hydrophobic face of the BH3 helix is buried in full-length Bak,³⁴ one possible explanation for the reduced binding of the longer Bak constructs is that the extra helices are occluding the hydrophobic residues required for binding to Bcl-x_L.

The effect of decreasing the length of the canonical Bak BH3 peptide (residues 72–87) was also examined systematically in order to determine the minimal peptide required for binding to Bcl-x_L (Fig. 5). While deletion of residues N86 and R87 [resulting in the Bak(72–85) peptide] led to a reduction in binding to nearly background levels, residues G72 and Q73 were found to be dispensable for binding. These results were somewhat obscured by the fact that the two amino acids immediately preceding the Bak peptide in the eCPX–Bak fusions are also glycine and glutamine. To ensure that binding to Bcl-x_L was due only to Bak(74–87), we constructed a version of the eCPX–Bak(74–87) protein in which the GQ sequence preceding the Bak peptide was changed to GG. This construct exhibited fluorescence equivalent to that observed with Bak(72–87) and Bak(74–87), indicating that G72 and Q73 are indeed dispensable for binding to Bcl-x_L.

Effect of Bak peptide length on Bcl-2 binding

Binding of the Bak(72–87) peptide to Bcl-2 has been previously observed using fluorescence polarization competition assays.²³ The affinity of Bak(72–87) for Bcl-2 is reported to be several-fold lower than that for Bcl-x_L ($K_d = 1.6 \mu\text{M}$ for Bcl-2; $K_d = 480 \text{ nM}$ for Bcl-x_L), and our system qualitatively captures this difference in affinity (Fig. 6). We also investigated the binding of the Bak(72–89) peptide to Bcl-2 and Bcl-x_L and surprisingly found that this peptide bound equally well to Bcl-2 and Bcl-x_L (Fig. 6). We next used these protein–peptide interactions as a test case for a novel method for the calculation of approximate binding affinities, K^* . The method consists of five steps: (i) structure prediction, (ii) clustering, (iii) docking simulation, (iv) ensemble generation, and (v) approximate binding affinity calculation (see Supplementary Materials and Methods for details on the computational approach). The same four complexes that were tested experimentally [Bak(72–87)–Bcl-x_L, Bak(72–89)–Bcl-x_L, Bak(72–87)–Bcl-2, and Bak(72–89)–Bcl-2] were investigated using the computational tool. Based on the orders of magnitude of the approximate binding affinities (Table 2), Bak(72–87) and Bak(72–89) bind with comparable apparent affinity to Bcl-x_L while the K^* values for these two peptides in complex with Bcl-2 differ by 8 orders of magnitude (see rightmost column of Table 2). These calculations are consistent with the experimental findings described above, specifically that Bak(72–87) and Bak(72–89) bind equally well to Bcl-x_L, but the affinity of Bak(72–89) for Bcl-2 significantly exceeds the affinity of Bak(72–87) for Bcl-2. Given that this computational method qualitatively captures the experimental results, the method may also prove useful in designing Bak variants with improved affinity.

Role of Arg88 and Tyr89 of Bak in Bcl-2 binding

To more deeply understand the increased binding of Bak(72–89) to Bcl-2 relative to Bak(72–87), we systematically mutated the Arg88 and Tyr89 residues in the Bak peptide to investigate the role of side-chain charge and size on the binding of Bak(72–89) to Bcl-2 (Table 3). Mutation of the positively charged Arg88 to Ala (R88A) reproducibly led to an increase in fluorescence relative to wild-type Bak(72–89). Mutations of Arg88 to a negatively charged amino acid (R88E) or a neutral, similarly sized amino acid (R88Q) were deleterious but not cata-strophic to the binding of Bak(72–89) to Bcl-2. If the fluorescence values obtained in these mutants are placed in rank order based on the identity of the residue in position 88, we obtain $A > R > Q > E$. This rank order coincides precisely with the amino acid order in the experimental helical propensity scale³⁵ when R and E are both charged. It has been previously noted that mutation of amino acids in a peptide derived from the BH3 region of the pro-apoptotic protein Bad to improve helical propensity led to increases in binding affinity of the peptide to Bcl-x_L.²⁰ We conclude that the high helical propensity of Arg88, rather than its positive charge, is responsible for the increased apparent affinity of the Bak(72–89) peptide relative to Bak(72–87). The bulky nature of the tyrosine side chain also appears to play a role in the binding of Bak(72–89) to Bcl-2 since its deletion or mutation to alanine has a deleterious effect on binding (Table 3).

Affinity maturation of Bak(72–87) for Bcl-x_L

Perhaps the most unique aspect of our binding platform is its ability to be adapted for high-throughput screening to identify Bak variants with improved binding characteristics. To illustrate this, we constructed a combinatorial library of Bak variants in which each of the four residues composing the hydrophobic face of the amphiphilic BH3 helix (V74, L78, I81, and I85) was allowed to change to a similar large, hydrophobic amino acid (L, V, I, M, and F). These residues were targeted because the hydrophobic face of the BH3 helix of Bak is critical in forming contacts with Bcl-x_L and we reasoned that gains in affinity could be realized by mutagenizing these positions. The decision to focus our library on only large hydrophobic amino acids was based on two considerations. First, a library consisting of four

positions randomized by the degenerate NTK codon contains only $8^4 = 4096$ members, ensuring that the entire sequence space of the library can be redundantly sampled by flow cytometry. Secondly, the BH3 region of the Bcl-2 class of proteins is very highly conserved,³⁶ and only hydrophobic amino acids are found in these positions in Bcl-2 class members (see Table 1 in Ref.³⁷).

Cells displaying library members were treated with a limiting amount of biotinylated Bcl-x_L (16 nM) and stained with SAPE as in the equilibrium binding studies described above. Cells transformed with the library exhibit a pronounced shoulder in the fluorescence data as compared to wild-type Bak(72–87) (Fig. S3), and these highly fluorescent members of the population were collected using fluorescence-activated cell sorting. Analysis of individuals from the sorted subpopulation revealed several distinct clones that retained high fluorescence (Table 4). Of particular note is that one sequence, mut7, appeared four times while each of the other three sequences was only observed once. Some sequence trends are observed in these clones: leucine frequently replaces valine in position 74, while leucine is somewhat retained in position 78. The substitution of leucine with methionine at position 78 is tolerated. Neither of the isoleucine residues in positions 81 and 85 is strongly retained, and Ile85 is always replaced with phenylalanine. The I81F mutation was previously observed in phage display studies to isolate miniature protein/Bak chimeras with high affinity to Bcl-2.³⁸ We observe the I81F mutation once, but leucine is more strongly preferred in position 81 in the clones found in our library. Of the four different sequences analyzed, mut7 and mut8 exhibited the highest fluorescence and were further characterized by an estimation of the K_d toward Bcl-x_L as described above. These variants exhibit a 3- to 4-fold increase in apparent affinity for Bcl-x_L over the wild-type Bak(72–87) peptide, with the best clone, mut8, exhibiting an apparent K_d lower than 50 nM (Table 4; Fig. S4). Interestingly, both mut7 and mut8 also exhibit improved binding to Bcl-2 as evidenced by equilibrium binding experiments (data not shown).

Conclusions

In this article, we describe a rapid, quantitative, flow-cytometry-based assay for studying the interactions between apoptotic proteins. Given that a 16-mer helical peptide corresponding to the BH3 region of Bak (amino acids 72–87) has been demonstrated to be sufficient for binding to Bcl-x_L, this assay was first applied to investigate the effect of Bak peptide length on Bcl-x_L binding. Significantly increasing the length of the Bak peptide beyond the BH3 region decreases its affinity for Bcl-x_L. Truncation analysis on the Bak (72–87) peptide revealed that residues 72 and 73 are dispensable for binding to Bcl-x_L, suggesting that the minimal Bak peptide for high-affinity binding to Bcl-x_L is composed of only 14 amino acids (amino acids 74–87). Surprisingly, we also find that an 18-mer Bak peptide corresponding to amino acids 72–89 binds equally well to Bcl-x_L and the related anti-apoptotic protein Bcl-2. These results illustrate that efforts toward generating paralog-specific binding peptides³⁹ can benefit from consideration of peptide length as well as sequence considerations. Finally, to demonstrate the engineering potential of our assay, we screened a saturation mutagenesis library of variants of Bak(72–87) for improved affinity to Bcl-x_L. Variants with a 3- to 4-fold decrease in apparent K_d were readily isolated from the library. The mutants selected from this screen include frequent substitutions of the isoleucine residues in positions 81 and 85 with phenylalanine, indicating that one potential strategy for increasing the affinity of the Bak peptide is to increase the steric bulk of the hydrophobic face of the C-terminal half of the peptide. It is anticipated that further gains in affinity, kinetic stability, and paralog specificity can be realized using this screening method.

Materials and Methods

Bacterial strains, reagents, and enzymes

All cell surface display experiments were performed in *E. coli* strain MC1061 [F^- *araD139* Δ (*ara-leu*)7696 *galE15 galK16* Δ (*lac*)X74 *rpsL* (Str^R) *hsdR2* ($r_k^- m_k^+$) *mcrA mcrB1*]. Large-scale protein expression was carried out in *E. coli* strain BL21(DE3) [F^- *ompT gal dcm lon hsdS_B* ($r_b^- m_b^+$) (DE3)]. Cloning steps were carried out in XL-1 Blue [*recA1, endA1, gyrA96, thi, hsdR17, supE44, relA1, lac*, (F' *proAB, lacI^q, lacZ* Δ M15, Tn10)]. Oligonucleotides were obtained from Integrated DNA Technologies. Restriction enzymes and T4 DNA ligase were purchased from New England Biolabs. PicoMaxx polymerase was from Agilent. Streptavidin R-phycoerythrin conjugate (SAPE) was purchased from Invitrogen. D-Biotin, anhydrotetracycline, and anti-His monoclonal antibody were purchased from Sigma. Lysozyme was obtained from USB. Antibiotics were used for plasmid maintenance at the following concentrations: ampicillin, 100 mg/L; kanamycin, 25 mg/L; and chloramphenicol, 25 mg/L.

Plasmids

Detailed information about plasmid and library construction can be found in Supplementary Materials and Methods. Plasmids for the cell surface display of Bak peptides were derived from pB33eCPX-SApep.³³ The gene encoding the Bak peptide was PCR-amplified from an *E. coli* codon-optimized Bak gene and inserted into the eCPX display system to generate N-terminal Bak fusions to eCPX. To facilitate Western blotting, we constructed C-terminally His-tagged versions of each Bak peptide-eCPX fusion. The Bak(72–87) saturation mutagenesis library was constructed with primers containing NTK (N: A,T,G, C; K: G,T) degenerate codons at the codons corresponding to Val74, Leu78, Ile81, and Ile85. Plasmids for the expression of Bcl-x_L and Bcl-2 were derived from the pASK75 vector.⁴⁰ The gene for C-terminally histidine-tagged Bcl-x_L (residues 1–210, Δ 46–85)¹⁹ was constructed by PCR amplifying two segments of a codon-optimized, full-length Bcl-x_L gene and assembling the fragments by overlap PCR. A sequence encoding an 18-amino-acid biotin acceptor peptide (MAGGLNDIFEAQKIEWHE, underlined lysine is the site of biotinylation)⁴¹ was appended to the 5' end of the Bcl-x_L gene described above to generate a gene encoding biotinylated Bcl-x_L. A previously described Bcl-2 chimera (isoform 2) that can be solubly expressed in *E. coli*²³ consists of residues 1–34 of Bcl-2, followed by residues 35–50 of Bcl-x_L and residues 92–207 of Bcl-2. The biotin acceptor peptide tag described above was added to the N-terminus of the chimera as was a C-terminal His-tag to facilitate purification.

Cell surface display of Bak-eCPX fusions

In a typical experiment, 100 μ L of an overnight culture of MC 1061 transformed with a vector encoding a Bak-eCPX fusion protein was subcultured in 10 mL of LB medium supplemented with chloramphenicol and grown to an OD₆₀₀ (optical density at 600 nm) of 0.6 with shaking at 37 μ C. The culture was induced by adding arabinose to a final concentration of 0.2% for 2.5 h at room temperature with cultures typically reaching a final OD₆₀₀ of 1.2. At this time, cells were subjected either to binding assays (described below) or to lysis and OMP. OMPs were isolated as previously described.^{42–44} OMPs were electrophoresed in 15% Tris-tricine gels at 140 V. Western blotting to detect Bak peptide-eCPX expression levels in OMPs was performed using an anti-His-horseradish peroxidase conjugate. Further details about Western blotting experiments can be found in Supplementary Information.

Expression and purification of biotinylated Bcl-x_L and Bcl-2

BL21(DE3) cells were cotransformed with a plasmid encoding either Bcl-x_L or Bcl-2 and pMON-BirA, which encodes a constitutively expressed bacterial biotin ligase. LB medium (1 L) supplemented with ampicillin and kanamycin was inoculated with 3 mL overnight culture and was incubated with shaking at 37 °C. When the OD₆₀₀ of the culture reached 0.2, 2 mg D-biotin was added. Upon reaching an OD₆₀₀ of 0.6, the culture was induced with anhydrotetracycline to a final concentration of 0.2 mg/L. The cells were harvested after 5 h of induction at room temperature and lysed by sonication and lysozyme treatment. The protein was purified using Ni-NTA affinity resin (Qiagen) according to the manufacturer's recommendation and buffer-exchanged into phosphate-buffered saline (PBS, pH 7.4) using 10 DG gel-filtration columns (Bio-Rad). Typical yields for biotinylated Bcl-x_L were 12–18 mg/L of culture while the yield of biotinylated Bcl-2 was typically only 1 mg/L of culture.

Binding assays and flow cytometry

Cells displaying Bak–eCPX fusions (1 mL culture) were collected by centrifugation at 6000g for 5 min and resuspended in 1 mL PBS. The cell suspension was diluted 10-fold to a final concentration of ~10⁸ cells/mL, and 50 µL of the suspension was incubated with purified Bcl-x_L or Bcl-2 at a final concentration of 1.6 µM. The mixture was incubated with mild rotation at room temperature for 1 h. The cells were subsequently collected by centrifugation and resuspended in 50 µL PBS. To this mixture, 50 µL of 100 nM SAPE was added and the cell suspension was incubated on ice for 30 min. The cells were centrifuged once more to remove unbound SAPE and resuspended in 2 mL PBS. Samples were immediately analyzed on a Partec CyFlow ML Flow Cytometer equipped with a 488-nm laser. Fluorescence data were measured in the FL2 channel (575 nm bandpass filter). Each set of binding assays was performed at least three times.

Binding isotherms and kinetic studies

To obtain equilibrium binding isotherms, we incubated cells displaying the Bak(72–87)–eCPX fusion with a range of concentrations of biotinylated Bcl-x_L from 1.66 nM to 8.34 µM. The median fluorescence of the cell population was determined using flow cytometry, and the data were fit to a single-site saturation model (see Supplemental Information) using MATLAB to obtain the apparent K_d . The dissociation rate constant k_{off} was measured by a competition assay. Cells displaying the Bak(72–87)–eCPX fusion were labeled with 1.6 µM biotinylated Bcl-x_L and SAPE as described above. The cells were subsequently treated with 41.5 µM untagged Bcl-x_L to act as a competitor. The median fluorescence of the cell population was measured using flow cytometry each minute for 8 min. The dissociation rate constant was calculated by fitting the data to an exponential decay model.

Library screening

Cells displaying the Bak(72–87) library were incubated with biotinylated Bcl-x_L and SAPE as described in Binding assays and flow cytometry except that Bcl-x_L was added to a final concentration of 16 nM. The top 1% of the cells in the FL2 channel was collected in single-cell mode on FACSVantage SE cell sorter in the Princeton University flow cytometry core facility. A portion of the sorted cells was plated on LB/chloramphenicol plates to facilitate analysis of individual members of the population.

Computational methods

The first step in calculating the approximate binding affinities is generating an ensemble of structures of the two Bak peptides. This is done using RosettaAbinitio.^{45–47} The sequences of each peptide are provided as input, and 1000 possible three-dimensional structures are generated per peptide. The 1000 structures are then clustered based upon the ϕ and ψ angles

using OREO,^{48,49} which groups together similar structures. The medoids from the 10 largest clusters, plus the overall-lowest energy structure, are selected for the docking simulation. This gives 11 backbone configurations for each of the Bak peptides. The solution structure of Bak(72–87) bound to Bcl-x_L [Protein Data Bank (PDB) code: 1BXL] was used as the starting structure for the Bcl-x_L docking simulations. Docking was done using RosettaDock.^{50–52} For the Bak(72–87)–Bcl-x_L complex, each of the 11 Bak(72–87) peptides was aligned to the structure of Bak(72–87) in complex with Bcl-x_L. For this case, since the native structure of Bak(72–87) was known, this peptide structure was used as the overall lowest-energy structure. For each of the 11 docking simulations, 1000 possible docked conformers were generated, and the 10 lowest-energy conformers from each of the simulations were selected for the final ensemble generation.⁵³ A similar procedure was carried out for the complex of Bak(72–89) and Bcl-x_L. In this case, a native structure of Bak(72–89) was not known; thus, the predicted lowest-energy structure from RosettaAbinitio was used. Since there was no crystal structure of Bcl-2 in complex with Bak, the apo structure of Bcl-2 was used (PDB code: 1G5M). This was aligned to the Bak (72–87)–Bcl-x_L complex, and the binding region was found to be structurally similar. The Bak(72–87)–Bcl-2 crystal structure was constructed by simply replacing Bcl-x_L with the aligned structure of Bcl-2. As described above, the Bak peptides were aligned to the native crystal structure of Bak(72–87) in complex with Bcl-2 and the docking simulations and ensemble generation were carried out.

Supplementary Material

Refer to Web version on PubMed Central for supplementary material.

Acknowledgments

We are grateful to Patrick Daugherty (University of California, Santa Barbara) for the gift of pB33eCPX-SApep and to Michael Diehl (Rice University) for pMON-BirA. We also thank Christina DeCoste for assistance with cell sorting. This work was supported by Princeton University startup funds to A.J.L. C.A.F. acknowledges support from the National Science Foundation (CTS-0426691), National Institutes of Health (R01 GM52032), and U.S. Environmental Protection Agency (GAD R832721-010).

Abbreviations used

eCPX	enhanced circularly permuted OmpX
SAPE	streptavidin–phycoerythrin
SPR	surface plasmon resonance
OMP	outer-membrane preparation
PBS	phosphate-buffered saline
PDB	Protein Data Bank

References

1. Hengartner MO. The biochemistry of apoptosis. *Nature* 2000;407:770–776. [PubMed: 11048727]
2. Cory S, Adams JM. The BCL2 family: regulators of the cellular life-or-death switch. *Nat Rev, Cancer* 2002;2:647–656. [PubMed: 12209154]
3. Walensky LD. BCL-2 in the crosshairs: tipping the balance of life and death. *Cell Death Differ* 2006;13:1339–1350. [PubMed: 16763614]
4. Youle RJ, Strasser A. The BCL-2 protein family: opposing activities that mediate cell death. *Nat Rev, Mol Cell Biol* 2008;9:47–59. [PubMed: 18097445]

5. Oltvai ZN, Milliman CL, Korsmeyer SJ. Bcl-2 heterodimerizes in vivo with a conserved homolog, Bax, that accelerates programmed cell death. *Cell* 1993;74:609–619. [PubMed: 8358790]
6. Chittenden T, Harrington EA, Oconnor R, Flemington C, Lutz RJ, Evan GI, Guild BC. Induction of apoptosis by the Bcl-2 homolog Bak. *Nature* 1995;374:733–736. [PubMed: 7715730]
7. Tsujimoto Y, Cossman J, Jaffe E, Croce CM. Involvement of the Bcl-2 gene in human follicular lymphoma. *Science* 1985;228:1440–1443. [PubMed: 3874430]
8. Boise LH, Gonzalezgarcia M, Postema CE, Ding LY, Lindsten T, Turka LA, et al. Bcl-X, a Bcl-2-related gene that functions as a dominant regulator of apoptotic cell death. *Cell* 1993;74:597–608. [PubMed: 8358789]
9. Wei MC, Zong WX, Cheng EHY, Lindsten T, Panoutsakopoulou V, Ross AJ, et al. Pro-apoptotic BAX and BAK: a requisite gateway to mitochondrial dysfunction and death. *Science* 2001;292:727–730. [PubMed: 11326099]
10. Chipuk JE, Green DR. How do BCL-2 proteins induce mitochondrial outer membrane permeabilization? *Trends Cell Biol* 2008;18:157–164. [PubMed: 18314333]
11. Li P, Nijhawan D, Budihardjo I, Srinivasula SM, Ahmad M, Alnemri ES, Wang XD. Cytochrome *c* and dATP-dependent formation of Apaf-1/caspase-9 complex initiates an apoptotic protease cascade. *Cell* 1997;91:479–489. [PubMed: 9390557]
12. Minn AJ, Kettlun CS, Liang H, Kelekar A, Vander Heiden MG, Chang BS, et al. Bcl-x(L) regulates apoptosis by heterodimerization-dependent and -independent mechanisms. *EMBO J* 1999;18:632–643. [PubMed: 9927423]
13. McDonnell TJ, Troncoso P, Brisbay SM, Logothetis C, Chung LWK, Hsieh JT, et al. Expression of the protooncogene Bcl-2 in the prostate and its association with emergence of androgen-independent prostate cancer. *Cancer Res* 1992;52:6940–6944. [PubMed: 1458483]
14. Castle VP, Heidelberger KP, Bromberg J, Ou XG, Dole M, Nunez G. Expression of the apoptosis-suppressing protein Bcl-2, in neuroblastoma is associated with unfavorable histology and N-Myc amplification. *Am J Pathol* 1993;143:1543–1550. [PubMed: 8256847]
15. Hague A, Moorghen M, Hicks D, Chapman M, Paraskeva C. Bcl-2 expression in human colorectal adenomas and carcinomas. *Oncogene* 1994;9:3367–3370. [PubMed: 7936663]
16. Castilla C, Congregado B, Chinchon D, Torrubia FJ, Japon MA, Saez C. Bcl-xL is overexpressed in hormone-resistant prostate cancer and promotes survival of LNCaP cells via inter action with proapoptotic Bak. *Endocrinology* 2006;147:4960–4967. [PubMed: 16794010]
17. Dole MG, Jasty R, Cooper MJ, Thompson CB, Nunez G, Castle VP. Bcl-X(L) is expressed in neuroblastoma cells and modulates chemotherapy-induced apoptosis. *Cancer Res* 1995;55:2576–2582. [PubMed: 7780971]
18. Lebedeva I, Rando R, Ojwang J, Cossup P, Stein CA. Bcl-xL in prostate cancer cells: effects of overexpression and down-regulation on chemosensitivity. *Cancer Res* 2000;60:6052–6060. [PubMed: 11085527]
19. Sattler M, Liang H, Nettesheim D, Meadows RP, Harlan JE, Eberstadt M, et al. Structure of Bcl-x(L)–Bak peptide complex: recognition between regulators of apoptosis. *Science* 1997;275:983–986. [PubMed: 9020082]
20. Petros AM, Nettesheim DG, Wang Y, Olejniczak ET, Meadows RP, Mack J, et al. Rationale for Bcl-x(L)/Bad peptide complex formation from structure, mutagenesis, and biophysical studies. *Protein Sci* 2000;9:2528–2534. [PubMed: 11206074]
21. Denisov AY, Chen G, Sprules T, Moldoveanu T, Beauparlant P, Gehring K. Structural model of the BCL-w–BID peptide complex and its interactions with phospholipid micelles. *Biochemistry* 2006;45:2250–2256. [PubMed: 16475813]
22. Oberstein A, Jeffrey PD, Shi YG. Crystal structure of the Bcl-X-L–beclin 1 peptide complex—beclin 1 is a novel BH3-only protein. *J Biol Chem* 2007;282:13123–13132. [PubMed: 17337444]
23. Petros AM, Medek A, Nettesheim DG, Kim DH, Yoon HS, Swift K, et al. Solution structure of the antiapoptotic protein bcl-2. *Proc Natl Acad Sci USA* 2001;98:3012–3017. [PubMed: 11248023]
24. Chen L, Willis SN, Wei A, Smith BJ, Fletcher JI, Hinds MG, et al. Differential targeting of prosurvival Bcl-2 proteins by their BH3-only ligands allows complementary apoptotic function. *Mol Cell* 2005;17:393–403. [PubMed: 15694340]

25. Willis SN, Chen L, Dewson G, Wei A, Naik E, Fletcher JI, et al. Proapoptotic Bak is sequestered by Mcl-1 and Bcl-x(L), but not Bcl-2, until displaced by BH3-only proteins. *Genes Dev* 2005;19:1294–1305. [PubMed: 15901672]
26. Hsu YT, Youle RJ. Nonionic detergents induce dimerization among members of the Bcl-2 family. *J Biol Chem* 1997;272:13829–13834. [PubMed: 9153240]
27. Petros AM, Olejniczak ET, Fesik SW. Structural biology of the Bcl-2 family of proteins. *Biochim Biophys Acta* 2004;1644:83–94. [PubMed: 14996493]
28. Daugherty PS. Protein engineering with bacterial display. *Curr Opin Struct Biol* 2007;17:474–480. [PubMed: 17728126]
29. Bessette PH, Rice JJ, Daugherty PS. Rapid isolation of high-affinity protein binding peptides using bacterial display. *Protein Eng Des Sel* 2004;17:731–739. [PubMed: 15531628]
30. Daugherty PS, Chen G, Olsen MJ, Iverson BL, Georgiou G. Antibody affinity maturation using bacterial surface display. *Protein Eng* 1998;11:825–832. [PubMed: 9796833]
31. Harvey BR, Georgiou G, Hayhurst A, Jeong KJ, Iverson BL, Rogers GK. Anchored periplasmic expression, a versatile technology for the isolation of high-affinity antibodies from *Escherichia coli*-expressed libraries. *Proc Natl Acad Sci USA* 2004;101:9193–9198. [PubMed: 15197275]
32. Rice JJ, Schohn A, Bessette PH, Boulware KT, Daugherty PS. Bacterial display using circularly permuted outer membrane protein OmpX yields high affinity peptide ligands. *Protein Sci* 2006;15:825–836. [PubMed: 16600968]
33. Rice JJ, Daugherty PS. Directed evolution of a biterminal bacterial display scaffold enhances the display of diverse peptides. *Protein Eng Des Sel* 2008;21:435–442. [PubMed: 18480093]
34. Moldoveanu T, Liu Q, Tocilj A, Watson M, Shore G, Gehring K. The X-ray structure of a BAK homodimer reveals an inhibitory zinc binding site. *Mol Cell* 2006;24:677–688. [PubMed: 17157251]
35. Pace CN, Scholtz JM. A helix propensity scale based on experimental studies of peptides and proteins. *Biophys J* 1998;75:422–427. [PubMed: 9649402]
36. Hardwick JM, Youle RJ. SnapShot: BCL-2 proteins. *Cell* 2009;138:404. [PubMed: 19632186]
37. Boersma MD, Sadowsky JD, Tomita YA, Gellman SH. Hydrophile scanning as a complement to alanine scanning for exploring and manipulating protein–protein recognition: application to the Bim BH3 domain. *Protein Sci* 2008;17:1232–1240. [PubMed: 18467496]
38. Chin JW, Schepartz A. Design and evolution of a miniature bcl-2 binding protein. *Angew Chem, Int Ed* 2001;40:3806–3809.
39. Gemperli AC, Rutledge SE, Maranda A, Schepartz A. Paralog-selective ligands for Bcl-2 proteins. *J Am Chem Soc* 2005;127:1596–1597. [PubMed: 15700967]
40. Skerra A. Use of the tetracycline promoter for the tightly regulated production of a murine antibody fragment in *Escherichia coli*. *Gene* 1994;151:131–135. [PubMed: 7828861]
41. Beckett D, Kovaleva E, Schatz PJ. A minimal peptide substrate in biotin holoenzyme synthetase-catalyzed biotinylation. *Protein Sci* 1999;8:921–929. [PubMed: 10211839]
42. Puente JL, Juarez D, Bobadilla M, Arias CF, Calva E. The *Salmonella* OmpC gene—structure and use as a carrier for heterologous sequences. *Gene* 1995;156:1–9. [PubMed: 7537703]
43. Xu ZH, Lee SY. Display of polyhistidine peptides on the *Escherichia coli* cell surface by using outer membrane protein C as an anchoring motif. *Appl Environ Microbiol* 1999;65:5142–5147. [PubMed: 10543834]
44. Link AJ, Tirrell DA. Cell surface labeling of *Escherichia coli* via copper(I)-catalyzed [3 + 2] cyclo-addition. *J Am Chem Soc* 2003;125:11164–11165. [PubMed: 16220915]
45. Lee MR, Baker D, Kollman PA. 2.1 and 1.8 angstrom average C-alpha RMSD structure predictions on two small proteins, HP-36 and S15. *J Am Chem Soc* 2001;123:1040–1046. [PubMed: 11456657]
46. Rohl CA, Baker D. De novo determination of protein backbone structure from residual dipolar couplings using Rosetta. *J Am Chem Soc* 2002;124:2723–2729. [PubMed: 11890823]
47. Rohl CA, Strauss CEM, Misura KMS, Baker D. Protein structure prediction using Rosetta. *Methods Enzymol* 2004;383:66–93. [PubMed: 15063647]

48. DiMaggio PA, McAllister SR, Floudas CA, Feng XJ, Rabinowitz JD, Rabitz HA. Biclustering via optimal re-ordering of data matrices in systems biology: rigorous methods and comparative studies. *BMC Bioinformatics* 2008;9:458. [PubMed: 18954459]
49. DiMaggio PA, McAllister SR, Floudas CA, Feng XJ, Rabinowitz JD, Rabitz HA. A network flow model for biclustering via optimal reordering of data matrices. *J Glob Optim.* in press. 10.1007/s10898-008-9349-z
50. Daily MD, Masica D, Sivasubramanian A, Somarouthu S, Gray JJ. CAPRI rounds 3–5 reveal promising successes and future challenges for RosettaDock. *Proteins: Struct Funct Bioinform* 2005;60:181–186.
51. Gray JJ, Moughon S, Wang C, Schueler-Furman O, Kuhlman B, Rohl CA, Baker D. Protein–protein docking with simultaneous optimization of rigid-body displacement and side-chain conformations. *J Mol Biol* 2003;331:281–299. [PubMed: 12875852]
52. Gray JJ, Moughon SE, Kortemme T, Schueler-Furman O, Misura KMS, Morozov AV, Baker D. Protein–protein docking predictions for the CAPRI experiment. *Proteins: Struct Funct Genet* 2003;52:118–122. [PubMed: 12784377]
53. Kuhlman B, Baker D. Native protein sequences are close to optimal for their structures. *Proc Natl Acad Sci USA* 2000;97:10383–10388. [PubMed: 10984534]

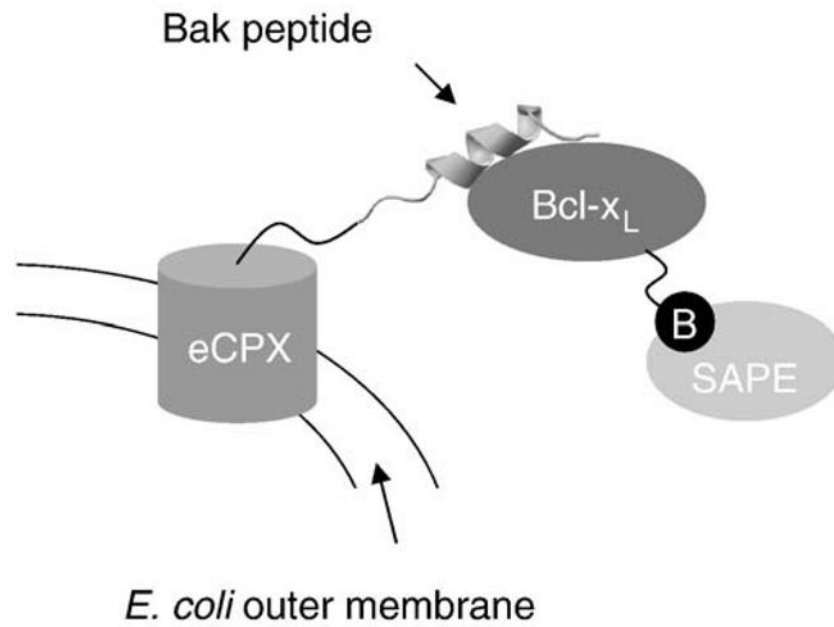


Fig. 1. Schematic of cell surface display platform for the detection of Bak–Bcl-x_L interactions. The eCPX protein localizes to the outer membrane of *E. coli* and displays a peptide fragment of Bak on the surface of the bacterium. Upon treatment of the cells with biotinylated Bcl-x_L and fluorescent streptavidin, cells with productive binding events will be rendered fluorescent and can be analyzed using flow cytometry. B, biotin; SAPE, streptavidin–phycoerythrin.

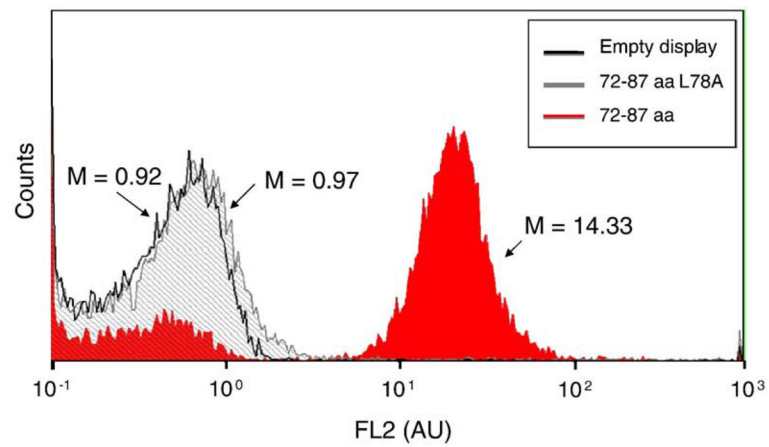


Fig. 2. Qualitative validation of binding platform with Bak(72–87) and Bcl-x_L. Cells displaying Bak(72–87) exhibit fluorescence ~15-fold higher than that of cells displaying no peptide. Mutation of the critical leucine in position 78 of the peptide to alanine abolishes binding.

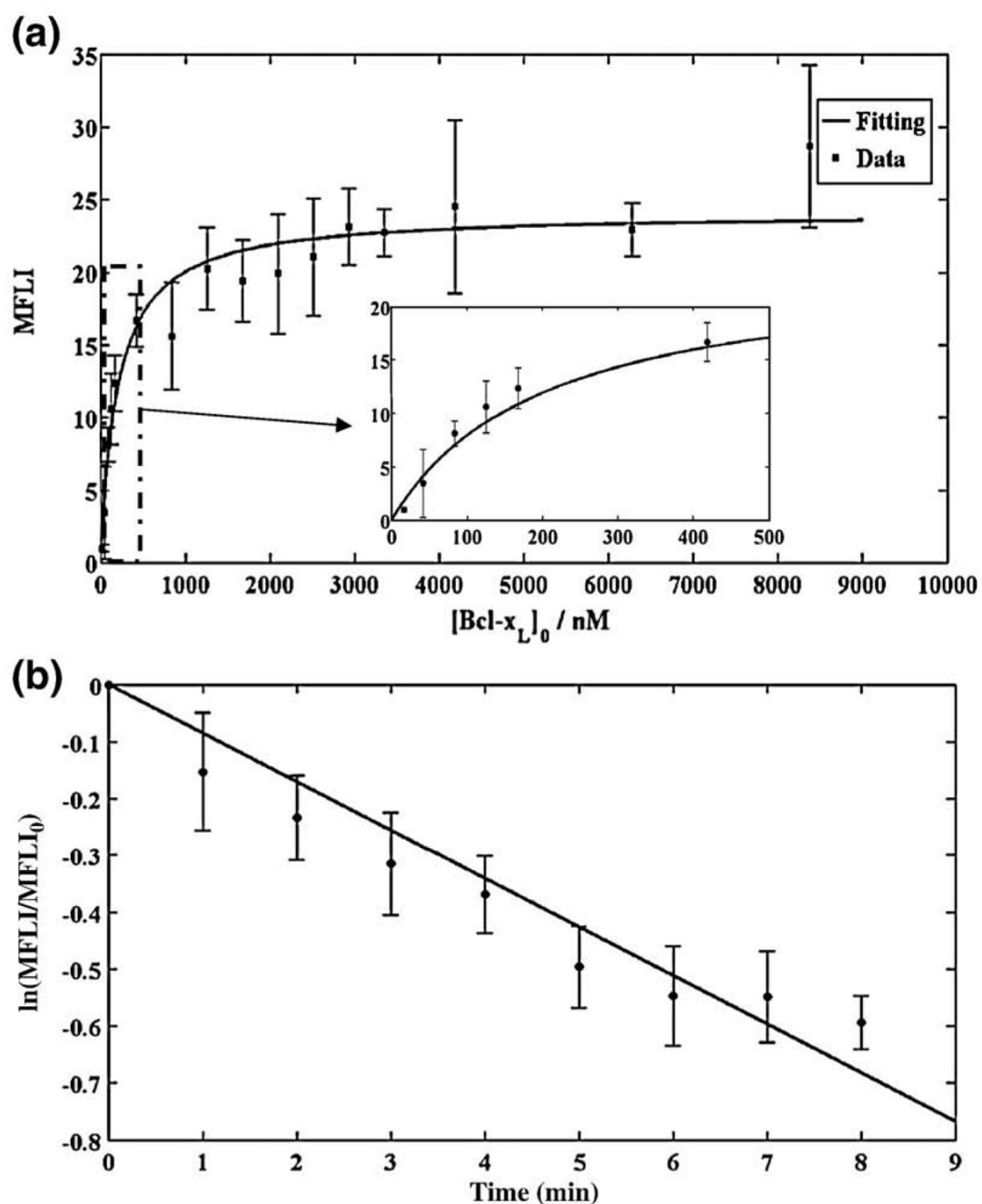


Fig. 3. Equilibrium binding isotherm and dissociation kinetics of the Bak(72–87)–Bcl-x_L interaction. (a) Binding isotherm generated by incubating cells displaying Bak (72–87) with different amounts of Bcl-x_L. The apparent K_d is 204 nM. Error bars represent the standard deviation of four independent experiments. The r^2 value for the fit is 0.93. MFLI, median fluorescence intensity. (b) Kinetics of dissociation of Bak(72–87) and Bcl-x_L measured by a competition assay. The apparent k_{off} is $1.42 \times 10^{-3} \text{ s}^{-1}$. Error bars represent the standard deviation of four independent measurements. The goodness of fit is $r^2 = 0.91$.

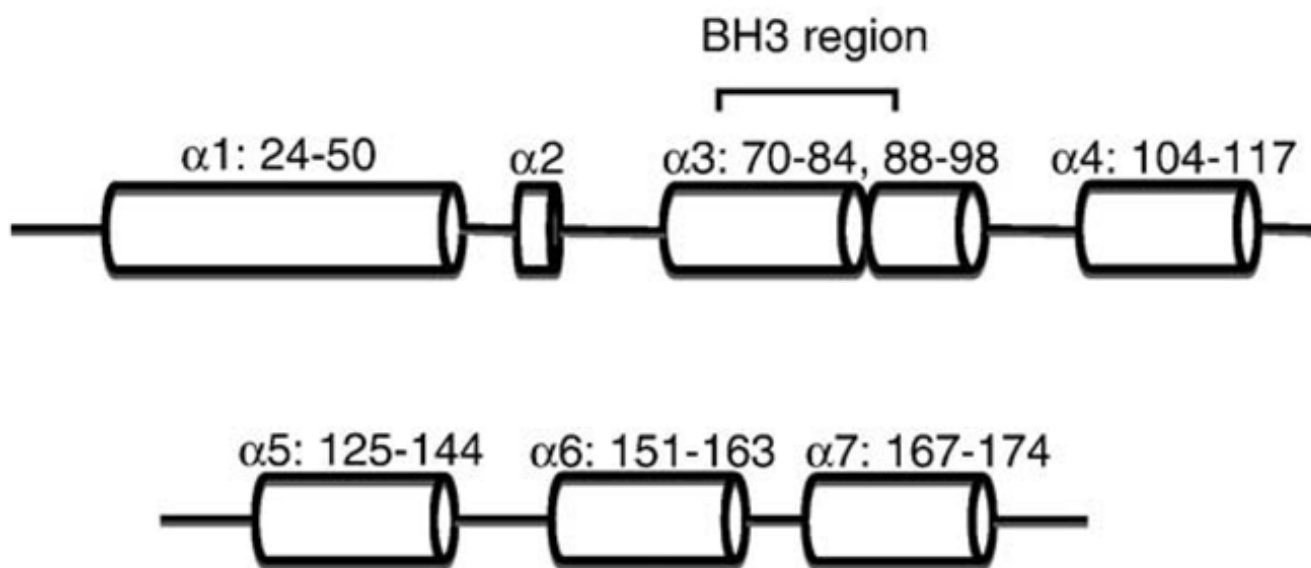


Fig. 4. Schematic of the secondary structure of Bak. The BH3 region is highlighted (following Ref. ³⁴ and PDB file 2IMS).

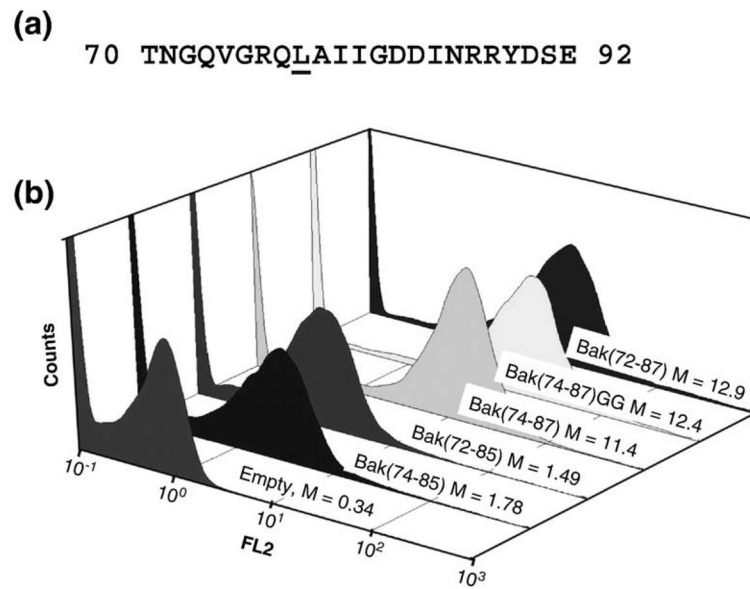


Fig. 5. Effect of truncation of Bak peptide on Bcl- x_L binding. (a) Sequence neighborhood of the BH3 region in Bak (amino acids 70–92). The critical leucine in position 78 is underlined as reference. (b) Fluorescence of truncation variants of Bak(72–87) peptide. Values displayed are median fluorescence of the cell population. Truncation of the C-terminus (residues 86 and 87) leads to a large decrease in binding while truncation of the N-terminus (residues 72 and 73) did not appreciably affect binding. Since the peptide linker connecting eCPX and the Bak peptide contains the sequence GQ immediately preceding the Bak peptide, a variant was constructed in which the GQ sequence was changed to GG, Bak(74–87) GG. This peptide bound Bcl- x_L equally as well as Bak(72–87).

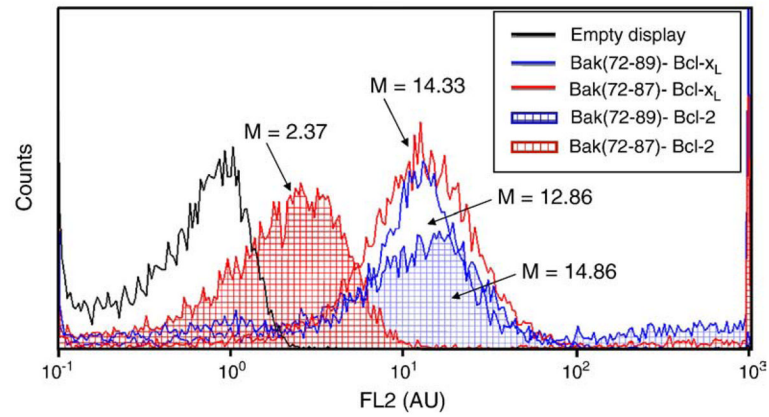


Fig. 6. Binding of Bak(72–89) to Bcl-x_L and Bcl-2. The Bak(72–87) peptide exhibits decreased binding to Bcl-2 relative to Bcl-x_L consistent with previous findings; however, Bak(72–89) binds equally well to Bcl-x_L and Bcl-2. M, median fluorescence of cell population.

Table 1Effect of Bak peptide length on Bcl-x_L binding

Construct	Median fluorescence (AU)
Empty eCPX	1.14
Bak(72–87)	21.29
Bak(70–93)	9.03
Bak(72–117)	1.54
Bak(24–89)	1.20
Bak(24–117)	1.20

Cells expressing Bak peptide–eCPX fusions were subjected to equilibrium binding with 1.6 μM Bcl-x_L, and the median fluorescence was measured via flow cytometry.

Table 2Approximate binding affinity K^* of Bak peptides complexed with Bcl-x_L and Bcl-2

Peptide	Protein	
	Bcl-x _L	Bcl-2
Bak(72-87)	1.24×10^{-1}	2.94×10^{-5}
Bak(72-89)	2.77×10^0	4.32×10^3

See the text for details on computational method for determining K^* .

Table 3

Role of R88 and Y89 side-chain charge and size on Bak(72–89) binding to Bcl-2

Construct	Mutation	Median fluorescence (AU)
Bak(72–87)	—	2.1
Bak(72–89)	—	19.1
Bak(72–89)	R88A	24.6
Bak(72–89)	R88E	8.4
Bak(72–89)	R88Q	11.1
Bak(72–89)	Y89A	11.9
Bak(72–88)	—	8.3

Table 4

Sequence and K_D of variants of Bak(72–87) with improved affinity to Bcl-xL

Clone	Times observed	Val74	Leu78	Ile81	Ile85	K_D (nM)
Wild type	—	V	L	I	I	204
mut7	4	L	L	L	F	66.5
mut8	1	L	L	F	F	47.7
mut10a	1	L	M	L	F	ND
mut10b	1	V	M	L	F	ND
Consensus	—	L	L	L	F	—

ND, not determined.